The Electrochemical and Biological Behaviour of Biomedical Alloy by Surface Modification Technique through E-Beam Evaporation

S. Gnanavel[1] · S. Ponnusamy[2] · J. Castro[3]

Abstract

Biomedical implants, especially the hip and knee implants, have been evolved over the years with great significance in terms of its biocompatibility and corrosion resistance. These implants, however, fail at their longevity when they encounter with the tissue, which is generally due to the failure in coatings over the surface of the implants. Moreover, coating procedures are very complex for applying them to three-dimensional implant structures. Hence to improve the coating property and make them easily applicable, we report a simple and realistic approach of Electron beam (E-beam) evaporation to modify the surface of the bio-metals (Ti–6Al–4V and 316L SS) with hydroxyapatite. The surface characterisation was done using SEM, XRD and AFM, which showed better thin film formation of hydroxyapatite (HA) on the metals. The potentiodynamic polarization and EIS measurements showed that hydroxyapatite-coated surfaces have better corrosion resistance than the bare metal substrates. The immersion study in SBF and cell viability using 3T3 cells proved that HA coated samples show better biomineralisation and better biocompatibility. Thus, HA deposition by E-beam evaporation over the metallic substrates can be applied as an effective surface modification technique for developing implant materials.

1 Introduction

Metallic biomaterials have been developed and extensively studied as implant materials over the past few decades. Various combinations of alloys were deployed and also commercially made available, especially as dental and orthopaedic implants [1–3]. Among them, Titanium and Stainless-steel alloys have proved great significance as implant material over the years [4–6]. Hydroxyapatite (HA, $(Ca_{10}(PO_4)_6(OH)_2)$, the major component of human hard tissues (65–70 wt%), is significant with high osteoconductivity, and has great ability to enhance bone ingrowth [7].

Numerous studies have been reported on HA coatings on Ti-based alloys and stainless-steel alloys [8].

Moreover, the bioactivity of HA deposited on the substrates depends upon the dissolution rate of the coating post-implantation, and if the coating has higher dissolution rates, it produces a higher concentration of Ca ions, which stimulates osteoblast activity and bone growth around the implant surface. The Ca/p ratio of the coated substrates post-implantation is proportional to the osseointegration of the implant [9]. Hence only very few studies have been reported on the Ca/P ratio of HA coated Ti–6Al–4V and 316L SS alloys as biomedical implants.

Various methods have been proposed for surface modification of Ti–6Al–4V, and 316L SS alloys like plasma spray coating [10], Ion beam deposition [11], Pulsed laser deposition [12], electrophoretic deposition, sol–gel derived coating [13]. These coating techniques which have great significance also have drastic limitations where plasma spray coating has low adhesion with limited wear resistance. These coatings resulted in non-uniform, inhomogeneous distribution over the substrate and lacked mechanical stability with the breakdown of the coating layer [14–16]. Hence a better realistic and

✉ S. Ponnusamy
   suruponnus@gmail.com

[1] Department of Biomedical Engineering, SRM Institute of Science and Technology, Chennai, Tamil Nadu, India

[2] Center for Materials Science and Nano Devices, SRM Institute of Science and Technology, Chennai, Tamil Nadu, India

[3] Department of Biomedical Engineering, University of Applied Sciences, Aachen, Germany

applicable method to achieve uniform deposition of HA over the substrate with Ca/P ratio similar to other coating methods is in great need to be established.

In this study, we report a Physical vapour deposition technique called E-beam evaporation method which is a benchtop setup that enables simplistic approach even to coat three-dimensional implants, which produce very thin and homogeneous coating over the substrate with higher mechanical stability and increased osteointegration [17, 18]. Furthermore, the coating parameters can be varied by the target material. Thus, this method can be an alternate deposition coating technique to produce thin films with a porous layer for better bone growth outside the implant surface.

2 Experimental Setup

2.1 Substrate Preparation

The substrates Ti–6Al–4V and 316L SS metals were cut into the following dimension ($10 \times 10 \times 3$) mm and polished using emery papers with grades up to 2000 in steps. The polished samples were cleaned using acetone and distilled water for 15 min, respectively via ultrasonicator and then dried for 15 min at room temperature.

2.2 Synthesis of HA and Deposition

HA can be prepared by using various methods in which the wet chemical precipitation method proves to be a very simple procedure. We synthesized HA according to previously established protocol [19], in short, 200 ml of DHP and CNT solution were prepared at pH 4 and 7.4 respectively. They were mixed and stirred overnight to obtain a precipitate which is cleaned with ethanol and dried in an oven at 80 °C. The pellet was made from the precipitate using a pressing machine with a thickness of 10 mm and sintered at 1200 °C for 6 h. The grain size can be controlled by pH and temperature, which was previously reported [20]. The polished and cleaned samples mentioned as Ti–6Al–4V and 316L SS were coated using the E-beam method with HA pellet as the target material at a distance of 15 cm. The deposition was done at a rate of 10 Å/S, and the pressure was maintained at 5×10^2 Torr.

2.3 Surface Characterization

The surface morphology and elemental analysis were carried using FESEM (FEI Quanta FEG 200), and the phase compositions of the coated metal were analysed using X-ray diffraction pan analytical X'Pert PRO with Cu Kα radiation ($\lambda = 1.542$ Å)]. The surface roughness of the coated and uncoated sample was determined by AFM (Easy scan2, Nano surf, Switzerland).

2.4 Biomineralisation and Cell Viability Analysis

The coated and uncoated substrates were immersed in 50 ml of freshly prepared simulated body fluid (SBF) which has similar ion concentrations of human plasma for 7 days at room temperature. The SBF was prepared as per the composition report previously [21]. After the immersion period, the surface morphology and elemental analysis of the substrates were done using electron microscopy. The cell viability was studied using MTT assay for the coated and uncoated (Ti–6Al–4V and 316L SS) substrates according to a previously established protocol [22]. In short, 3T3 cells cultured in DMEM (Dulbecco's Modified Eagle's Medium) supplemented with 10% FBS (Fetal Bovine Serum), 100 µg/ml streptomycin and 100 µg/ml were harvested, trypsinised and seeded on to a well plate containing the metal substrates at a density of 0.5×10^6 cells/ml and incubated for 24 h at 37 °C. Finally, the MTT Reagent was added to wells and incubated for 4 h after which the wells were aspirated to remove the medium. The absorbance was calculated using a microplate reader, and the cell viability was calculated from the data.

2.5 Electrochemical Measurements

Potentiodynamic polarization was done using Bio-logic VSP potentiostat/frequency response analysis system to evaluate the electrochemical behaviour of the samples. Three electrode systems with reference, standard and working electrode as substrate were used for the measurements. Before the beginning of Polarization procedure, the substrates were kept in SBF for 60 min to attain the open circuit potential (E_{ocp}). EIS measurements were performed at open circuit potential where a sine wave of 10 mV was applied. The spectra was acquired in a range of 100 kHz to 10 MHz. Impedance spectra were represented in both complex impedance diagrams (Nyquist and Bode plots). The E_{corr} and I_{corr} were obtained from Tafel Plots, and the corrosion current is explained by Stern–Geary equation [23]. The schematic representation of steps involved hydroxyapatite coated on biomedical alloys are show in Fig.1.
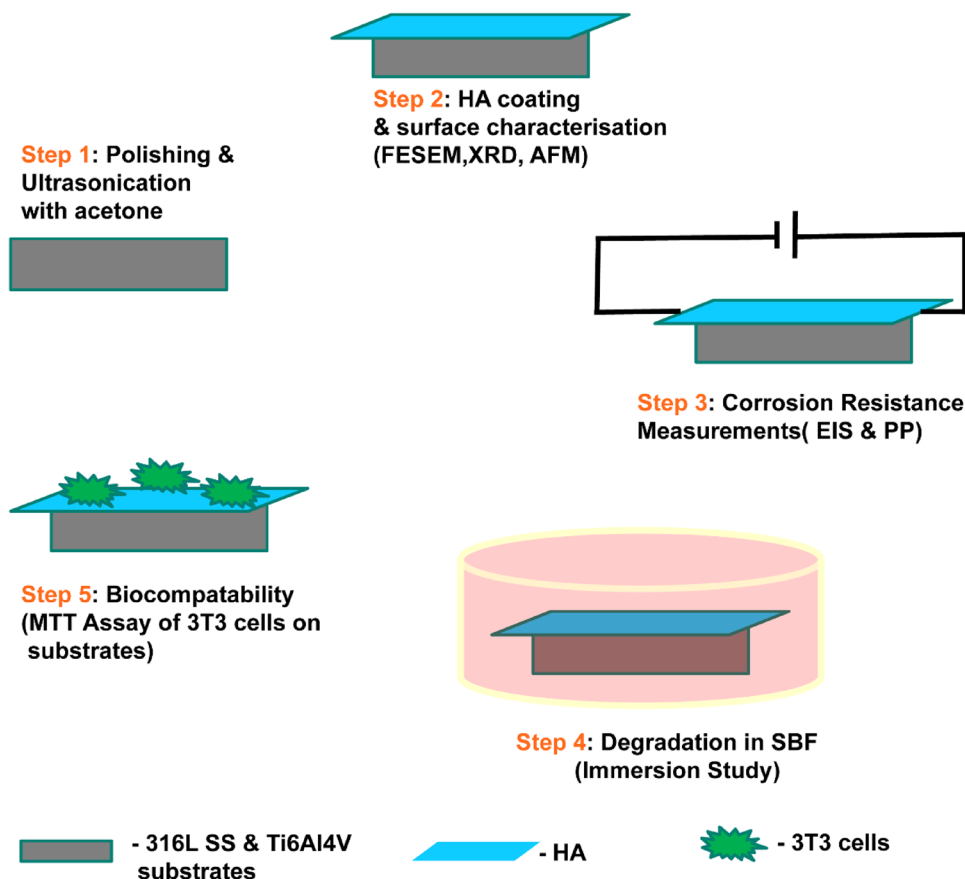
$$I_{corr} = (\beta a \times \beta c)/2.3Rp\,(\beta a + \beta c) \tag{1}$$

3 Results

3.1 Surface Morphology

The morphological characterisation of substrates by FESEM of HA coated, and uncoated samples are shown in Fig. 2. The coated substrates (Fig. 2b, e) have evidence of deposition of HA uniformly over the surface, which is denoted by EDS spectra where Ca and P peaks are

Fig. 1 Schematic diagram of steps involved in hydroxyapatite coated on titanium and 316L stainless steel

Step 1: Polishing & Ultrasonication with acetone

Step 2: HA coating & surface characterisation (FESEM,XRD, AFM)

Step 3: Corrosion Resistance Measurements(EIS & PP)

Step 5: Biocompatability (MTT Assay of 3T3 cells on substrates)

Step 4: Degradation in SBF (Immersion Study)

- 316L SS & Ti6Al4V substrates　　　- HA　　　- 3T3 cells

significantly visible. HA coated Ti–6Al–4V and 316L SS substrates show uniform deposition over the surface due to the substrate characteristics and change in the state of HA during deposition. Tables 1 and 2 details the elemental compositions present on the coated substrates. Ti–6Al–4V and 316L SS substrates show a higher percentage of oxygen 51.24% and 55.78% respectively along with Calcium deposition amounting up to 16.56% for Ti–6Al–4V and 19.21% for 316L SS. Phosphorous depositions over the substrates were 8.67% for Ti–6Al–4V and 9.64% for 316L SS substrates.

Three-Dimensional AFM images of HA coated Ti–6Al–4V, and 316L SS substrates are shown in Fig. 3a, b. The average roughness (Ra) of the coated substrates was 83.24 nm for Ti–6Al–4V and 96.11 nm for 316L stainless steel. The coated substrates reported an increased roughness than the uncoated substrates. The XRD pattern of the HA coated on Ti–6Al–4V and 316L SS alloy is shown in the Fig. 3c and d. It is observed from Fig 3d, that the strong peaks at 39.60°, 34.41° and 55.02° confirm the presence of hydroxyapatite and it well matches with JCPDS Card Number #090-0432 [24]. Similarly, the highest peaks at 38.16°, 41.23° and 54.01° represent the titanium substrate and it corresponds to JCPDS Card Number #44-1294). From the Fig. 3c, the strong peaks at

32.75°,45.17° and 51.17° confirmed the hydroxyapatite and it well matches with JCPDS Card Number #090-0432. The peaks at 44.24° and 91.08° represent the 316L substrate and it confirm with reference JCPDS Card Number #03-30,397. The presence of hydroxyapatite in the metal surface leads to improved biological response of implants. [24].

3.2 Immersion Study and Cell Viability

The coated substrates were immersed seven days in simulated body fluid solution (SBF) and imaged using FESEM with EDS spectra are shown in Fig. 4a–d. The elemental composition of the substrates obtained after the immersion is mentioned in Tables 3 and 4. The coated samples show calcium phosphate deposits, which can be visually seen as dense white spherical crystals over the substrates. The percentage of Calcium was 17.06% for Ti–6Al–4V and 15.31% for 316L SS substrates. The presence of phosphorous deposits was confirmed as it amounted to a total percentage of 7.88% and 7.98% for Ti–6Al–4V and 316L SS respectively. Figure 4e shows the in vitro cytotoxicity in terms of cell viability for 3T3 cells cultured in the extraction media of the coated samples for 24 h. The viability was measured as the ability of live cells to convert MTT

Fig. 2 FESEM images of 316L SS and Ti–6Al–4V uncoated substrates (**a**) and (**d**), HA coated substrates (**b**) and (**e**) EDS spectra of HA coated substrates (**c**) and (**f**)
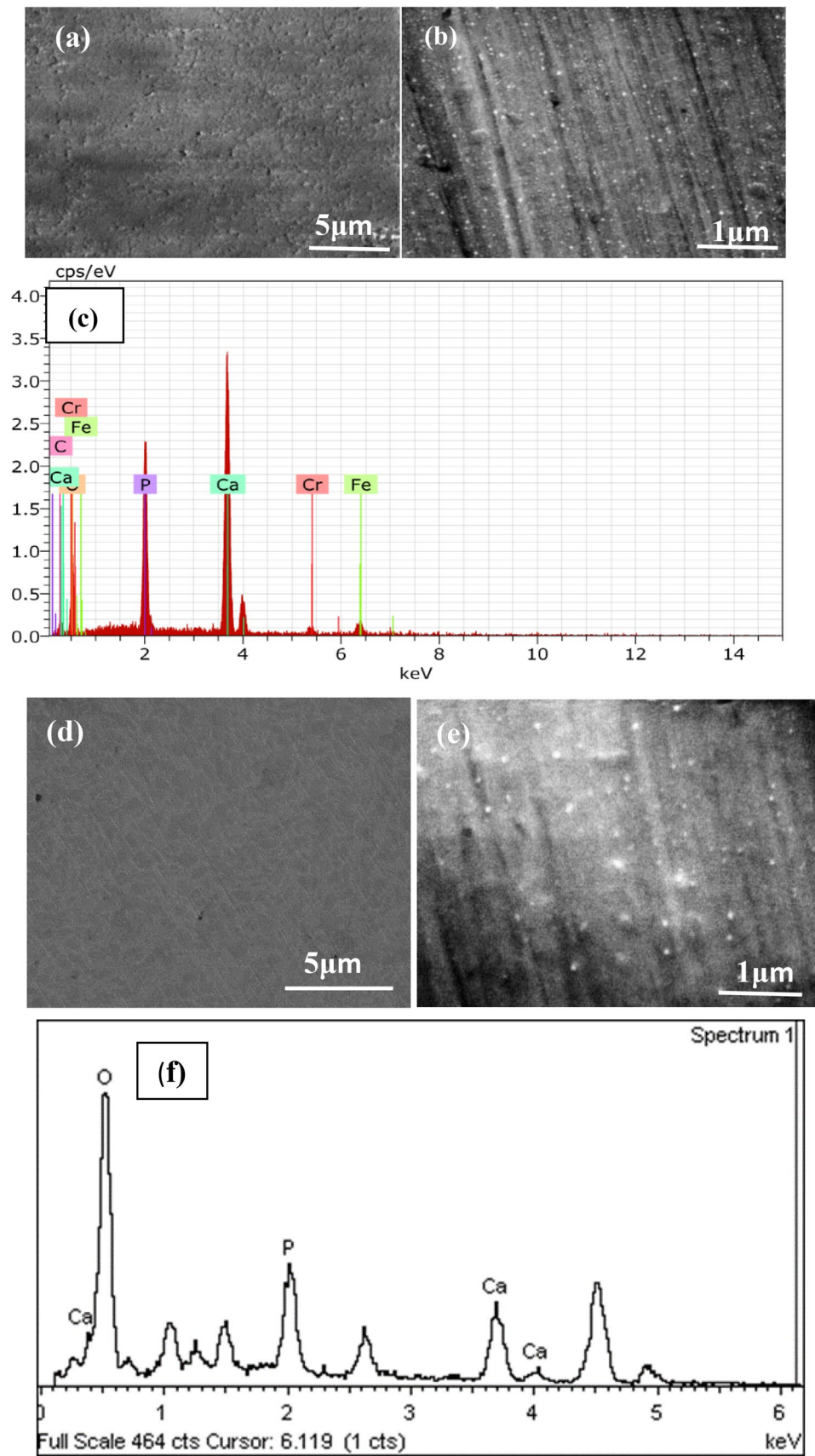
Table 1 Elemental composition of HA coated Ti–6Al–4V

Elements	Atomic number	Atomic %
O	8	51.24
Ca	20	16.56
P	15	8.67

Table 2 Elemental composition of HA coated 316L SS

Elements	Atomic number	Atomic %
O	8	55.78
Ca	20	19.21
P	15	9.64
Fe	26	1.75
C	6	11.56
Cr	24	0.64

into purple colour formazan whereas they are absorbed in a wavelength of 570 nm. The readings obtained were calculated for cell viability as a ratio of live cells per total cells seeded. Thus HA coated Ti–6Al–4V substrate shows better viability of 70% than the 316L substrates, which showed the viability of 50.1%.

3.3 Corrosion Properties

The potentiodynamic polarization curves are shown in Fig. 5a, b. The corresponding electrochemical parameters E_{corr} and i_{corr} values of HA coated, and uncoated Ti–6Al–4V and 316L SS substrates are summarized in Table 5. Generally, the corrosion current density i_{corr} is the important factor which is directly proportional and determines the corrosion resistance of the substrate. The coated Ti–6Al–4V has i_{corr} of 0.006 and 316L SS has a corrosion density current value of 0.0034 lower values than the uncoated substrates hence having higher corrosion resistance. The electrical impedance of the coated substrates is shown in Fig. 5c–f. The relation between the log (f) and log (Z) has a linear slope. The Nyquist plot in Fig. 5c and e has a semicircular curve with a larger diameter for the HA coated substrates when compared with that of the uncoated substrates [25]. The HA coated substrates have more impedance than that of the uncoated alloys.

4 Discussion

The SEM images show little white spots on the coated substrates, which indicates the deposition of HA particles on the surface, thereby enhancing the surface roughness for better implant fixation [26]. Moreover, the EDS spectra, which denote the presence of Ca and P peaks and the overall weight percentage, confirm the deposition of HA onto the substrates. However, Ti–6Al–4V and 316L SS substrates show fewer traces of Ti, Al and Fe, Cr compositions respectively, which can be contributed due to the thickness of HA over the substrate's surface. The roughness of the HA coated substrates by various deposition techniques generally varies from 20 to 90 nm [27]. Hence the roughness of Ti–6Al–4V and 316L SS about 17.81 nm and 17.24 nm is close to an acceptable range of roughness which promotes better endothelization. Generally, the increase in surface roughness can induce better endothelial coverage and osseointegration post-implantation [28]. The XRD pattern shows strong peaks of HA over both the substrate's surface between 30° to 60° which matches with the JCPDS file # (90432) as well titanium that has a peak at 38.16° JCPDS file # (44129) and 316L at 42.5° (30397).

The immersion studies showed that coated substrates have a Ca/P ratio of around 1.91 for 316L SS and 2.1 for Ti–6Al–4V, which promotes better biomineralization [29]. The HA coated Ti–6Al–4V, and 316L SS substrate, has deposits of Ca and P after the immersion in SBF similar to the percentages before immersion but with an increase in number, which denote promotion of biomineralisation over the substrate surface [30]. Moreover, the 316L SS substrate which noted for its low carbon content [31] exhibited traces of C after the immersion amounting to 20% of the total deposition which suppressed the peaks of Fe and Cr which was visible before the immersion in SBF. The cell viability of the coated substrates was calculated for 24 h after culturing the cell onto the substrates. There was reduced viability seen between coated and uncoated substrates by at least 10%. Hence prolonged exposure to cells may reduce the viability of the uncoated substrates, which can be attributed by the degradation and corrosion products released from the uncoated substrates which can be suppressed HA deposits over the surface [32].

While summarizing the corrosion properties of the coated and uncoated, HA deposits over the substrates, plays a major role in the anti-corrosion ability of the substrates. It is clear that the coated substrates have decreased corrosion rates with large capacitive loops, more positive (E_{corr}) value with
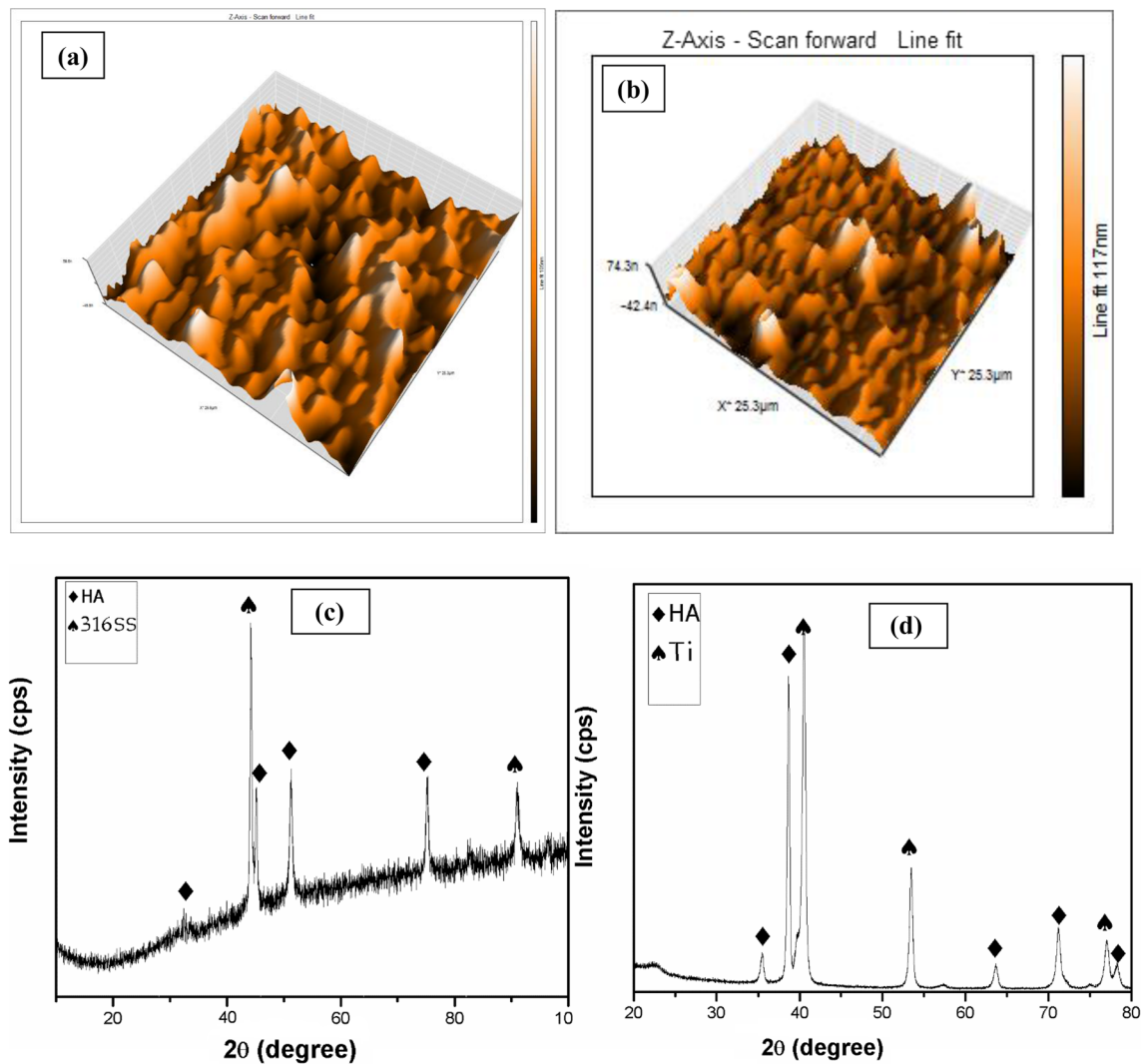
Fig. 3 AFM images of HA coated 316L SS substrate (**a**), Ti–6Al–4V substrate (**b**), XRD patterns of HA deposited on 316L SS (**c**), Ti–6Al–4V (**d**) substrates

lower (i_{corr}) values. The frequency and impedance of the HA coated substrates behave as an ideal capacitor, which means more barrier on the surface of the HA coated substrates than the uncoated substrates enabling them less prone to form cavities in a physiological environment preventing them from exposing their surface towards corrosion.

5 Conclusion

Hence the surface morphological and elemental characterisation results suggest that HA coating through E-beam evaporation could be achieved on metallic biomaterials similar to other complex techniques. The E-beam method as an alternative for coating implant surfaces provides better adhesion layer and a thin uniform coating over the surfaces, which are evident from the surface characterisation analysis. However, the thickness of the coating can be improvised based on the application. The layer thickness plays a major role in the mechanical stability and corrosion protection of
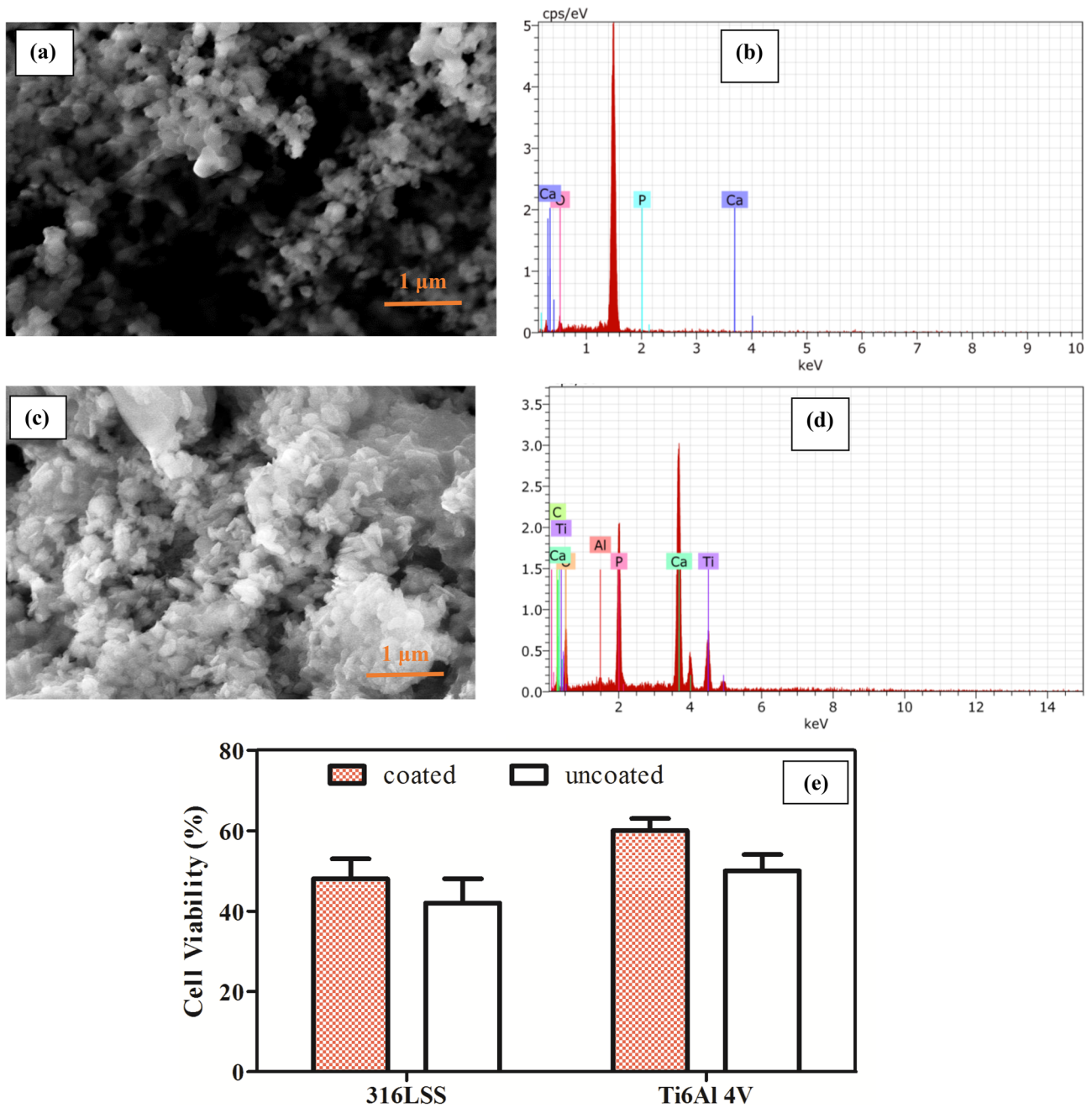
Fig. 4 FESEM images of HA coated 316L ss substrate (**a**), Ti–6Al–4V substrate (**c**) after immersion in SBF for 7 days and their corresponding EDS spectra 316L SS (**b**), Ti–6Al–4V (**d**). Cell viability of 3T3 cells cultured on substrates (**e**)

Table 3 Elemental composition of HA coated Ti–6Al–4V after immersion in SBF

Elements	Atomic number	Atomic %
O	8	52.54
Ca	20	17.06
C	6	16.53
P	15	7.88
Ti	22	5.46
Al	13	0.53

Table 4 Elemental composition of HA coated 316L SS after immersion in SBF

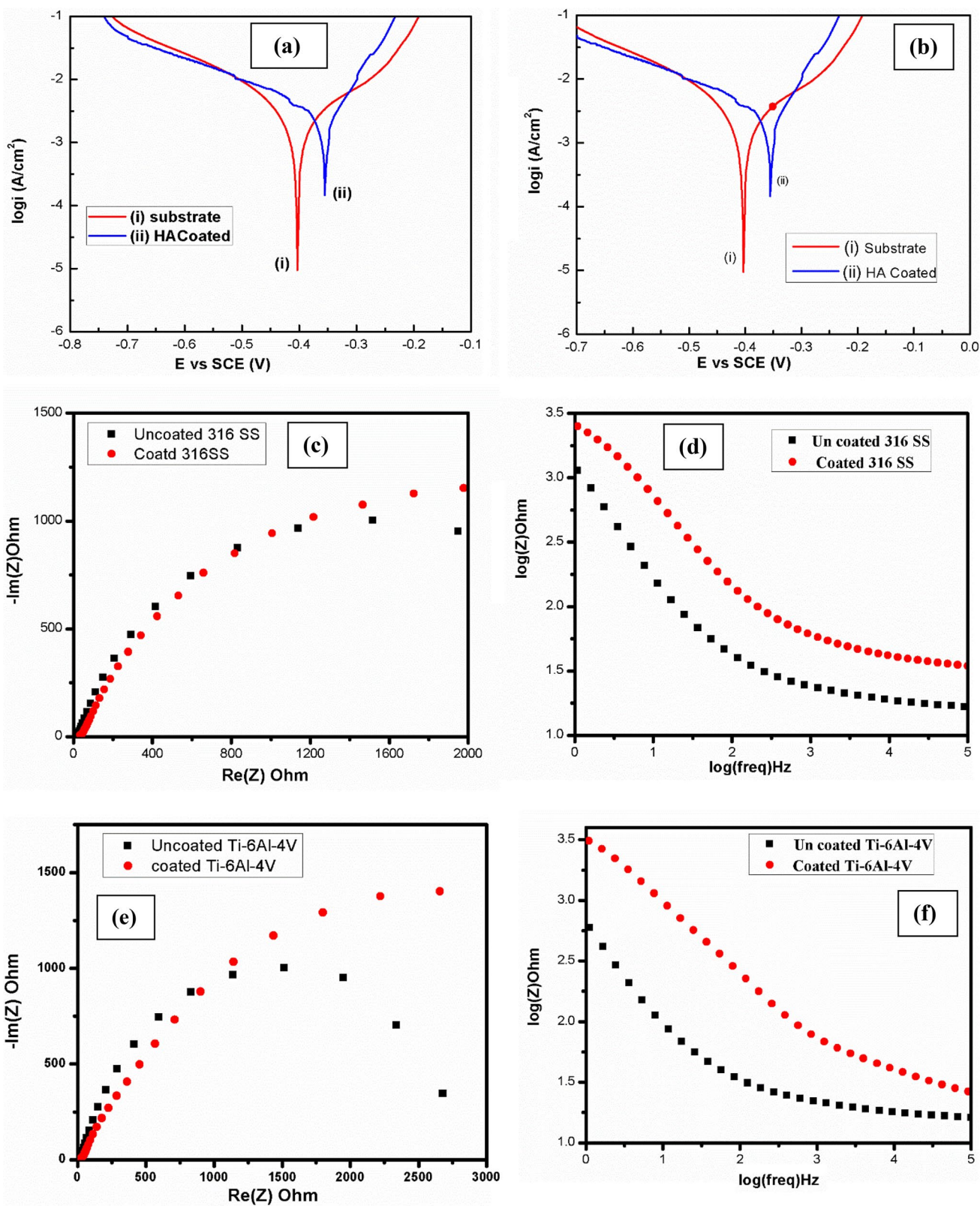| Elements	Atomic number	Atomic %
O	8	51.74
Ca	20	15.31
C	6	20.38
P	15	7.98

Fig. 5 Potentiodynamic polarization plots of HA coated, and uncoated 316L SS substrate (**a**) and Ti–6Al–4V substrate (**b**), EIS measurements Nyquist plots of HA coated 316L SS substrate (**c**), Ti–6Al–4V substrate (**e**), Bode plots of 316L SS substrate (**d**) and Ti–6Al–4V substrate (**f**)

Table 5 E_{corr} and i_{corr} values of HA coated and uncoated Ti–6Al–4V and 316L SS substrates

Substrates	E_{corr} (V)	i_{corr} (μA cm^2)
316L SS uncoated	-0.4	0.2345
316L SS coated	-0.346	0.0034
Ti–6Al–4V uncoated	-0.412	0.3456
Ti–6Al–4V coated	-0.358	0.006

the coating. The immersion of HA coating in SBF also indicates the formation of Calcium phosphate deposits over the substrate surface, which can facilitate osteointegration when applied to implant materials. Moreover, this being a primary study the coated substrates have better cell viability, but the overall viability can be improved, providing analysing live/dead cells in the follow-up studies for a higher cell growth period. However, by the results of the HA deposition by an easily applicable method, E-beam evaporation could be effectively used for coating of implant surfaces.

References

1. Chen Q, Thouas GA (2015) Metallic implant biomaterials. Mater Sci Eng 87:1–57
2. dos Santos V, Brandalise RN, Savaris M (2017) Metallic biomaterials. Engineering of biomaterials. Springer, Cham, pp 17–28
3. Park J, Lakes RS (2007) Biomaterials an introduction, 3rd edn. Springer, Berlin
4. Karimi S, Nickchi T, Alfantazi AM (2012) Long-term corrosion investigation of AISI 316L, Co–28Cr–6Mo, and Ti–6Al–4V alloys in simulated body solutions. Appl Surf Sci 258(16):6087–6096
5. Gepreel MAH, Niinomi M (2013) Biocompatibility of Ti-alloys for long-term implantation. J Mech Behav Biomed Mater 20:407–415
6. Al-Mobarak NA (2008) Comparative study of some metallic biomaterials used as implants. Materialwissenschaft und Werkstofftechnik: Entwicklung, Fertigung, Prüfung, Eigenschaften und Anwendungen technischer Werkstoffe 39(7):486–491
7. Bourgeois B, Laboux O, Obadia L, Gauthier O, Betti E, Aguado E, Bouler JM et al (2003) Calcium-deficient apatite: a first in vivo study concerning bone ingrowth. J Biomed Mater Res Part A 65(3):402–408
8. Lin JC, Kuo KH, Ding SJ, Ju CP (2001) Surface reaction of stoichiometric and calcium-deficient hydroxyapatite in simulated body fluid. J Mater Sci 12(8):731–741
9. Family R, Solati-Hashjin M, Nik SN, Nemati A (2012) Surface modification for titanium implants by hydroxyapatite nanocomposite. Caspian J Intern Med 3(3):460
10. Lu YP, Li MS, Li ST, Wang ZG, Zhu RF (2004) Plasma-sprayed hydroxyapatite + titania composite bond coat for hydroxyapatite coating on titanium substrate. Biomaterials 25(18):4393–4403
11. Palangadan R, Sukumaran A, Fernandez FB, John A, Varma H (2014) Pulsed laser deposition and in vitro characteristics of triphasic–HASi composition on titanium. J Biomater Appl 28(6):849–858
12. Kwok CT, Wong PK, Cheng FT, Man HC (2009) Characterization and corrosion behavior of hydroxyapatite coatings on Ti–6Al–4V fabricated by electrophoretic deposition. Appl Surf Sci 255(13–14):6736–6744
13. Sato M, Slamovich EB, Webster TJ (2005) Enhanced osteoblast adhesion on hydrothermally treated hydroxyapatite/titania/poly (lactide-co-glycolide) sol–gel titanium coatings. Biomaterials 26(12):1349–1357
14. Juliadmi D, Fauzi VR, Gunawarman G, Nur H, Idris MH (2017) Hydroxyapatite coating on titanium alloy Ti-6Al-4V with Electrophoretic Deposition (EPD) for Dental Root Application. Int J Adv Sci Eng Inf Technol 7(6):2152–2158
15. Kuroda K, Okido M (2012) Hydroxyapatite coating of titanium implants using hydroprocessing and evaluation of their osteoconductivity. Bioinorganic Chem Appl. https://doi.org/10.1155/2012/730693
16. Rattan PV, Sidhu TS, Mittal M (2012) An overview of hydroxyapatite coated titanium implants. Asian J Eng Appl Technol 1(2):40–43
17. Lee EJ, Lee SH, Kim HW, Kong YM, Kim HE (2005) Fluoridated apatite coatings on titanium obtained by electron-beam deposition. Biomaterials 26(18):3843–3851
18. Lee SH, Kim HE, Kim HW (2007) Nano-sized hydroxyapatite coatings on Ti substrate with TiO2 buffer layer by E-beam deposition. J Am Ceram Soc 90(1):50–56
19. Prema D, Gnanavel S, Anuraj S, Gopalakrishnan C (2018) Synthesis and characterization of different chemical combination of hydroxyapatite for biomedical application. Mater Today 5(2):8868–8874
20. Sun L, Berndt CC, Gross KA, Kucuk A (2001) Material fundamentals and clinical performance of plasma-sprayed hydroxyapatite coatings: a review. J Biomed Mater Res 58(5):570–592
21. Mohan L, Durgalakshmi D, Geetha M, Narayanan TS, Asokamani R (2012) Electrophoretic deposition of nanocomposite (HAp + TiO$_2$) on titanium alloy for biomedical applications. Ceram Int 38(4):3435–3443
22. Gnanavel S, Ponnusamy S, Mohan L (2018) Biocompatible response of hydroxyapatite coated on near-β titanium alloys by E-beam evaporation method. Biocatal Agric Biotechnol 15:364–369
23. Castro J, Krishnan KG, Jamaludeen S, Venkataragavan P, Gnanavel S (2017) Degradation and corrosion behavior of electrospun PHBV coated AZ-31 magnesium alloy for biodegradable implant applications. J Bio- Tribo- Corros 3(4):52
24. Gnanavel S, Ponnusamy S, Mohan L, Muthamizhchelvan C (2018) In vitro corrosion behaviour of Ti–6Al–4V and 316L stainless steel alloys for biomedical implant applications. J Bio- Tribo-Corros 4(1):1
25. Souto RM, Laz MM, Reis RL (2003) Degradation characteristics of hydroxyapatite coatings on orthopaedic TiAlV in simulated physiological media investigated by electrochemical impedance spectroscopy. Biomaterials 24(23):4213–4221
26. Shalabi MM, Gortemaker A, Hof MVT, Jansen JA, Creugers NHJ (2006) Implant surface roughness and bone healing: a systematic review. J Dent Res 85(6):496–500
27. Jafari S, Atabaki MM, Idris J (2012) Comparative study on bioactive coating of Ti-6Al-4V alloy and 316L stainless steel. Assoc Metall Eng Serbia 669(5):71
28. Paital SR, Dahotre NB (2009) Calcium phosphate coatings for bio-implant applications: materials, performance factors, and methodologies. Mater Sci Eng 66(1–3):1–70
29. Narayanan R, Seshadri SK, Kwon TY, Kim KH (2008) Calcium phosphate-based coatings on titanium and its alloys. J Biomed Mater Res Part B 85(1):279–299
30. Sewing A, Lakatos M, Scharnweber D, Roessler S, Born R, Dard M, Worch H (2004) Influence of Ca/P ratio on electrochemical assisted deposition of hydroxyapatite on titanium. Key engineering materials. Trans Tech Publications, Zurich, pp 419–422

31. Xavier SA, Vijayalakshmi U (2018) Electrochemically grown functionalized-Multi-walled carbon nanotubes/hydroxyapatite hybrids on surgical grade 316L SS with enhanced corrosion resistance and bioactivity. Colloids Surf, B 171:186–196

32. Clavell RS, de Llano JM, Carda C, Ribelles JG, Vallés-Lluch A (2016) In vitro assessment of the biological response of Ti–6Al–4V implants coated with hydroxyapatite microdomains. J Biomed Mater Res Part A 104(11):2723–2729